Titan Ballute Aerocapture Using a Perturbed TitanGRAM Model

Wyatt R. Johnson*
and Dan T. Lyons*
Jet Propulsion Laboratory, Pasadena, CA, 91007

Aerocapture using a towed, inflatable ballute system has been shown to provide significant performance advantages compared to traditional technologies, including lower heating rates and accommodation of larger navigational uncertainties. This paper extends previous results by designing a ballute aerocapture separation algorithm that can operate in a more realistic Titan atmospheric model based on TitanGRAM. This model incorporates both latitudinal variability as well as noisiness in the density profile.

I. Introduction

AEROCAPTURE can potentially significantly lower the propulsive delta-V costs for capturing a spacecraft into orbit about a destination body. Many studies have been made to investigate the feasibility of aerocapture using a variety of techniques, such as a ballistic unguided entry, or using some form of lift or drag modulation to help control the spacecrafts atmospheric trajectory to achieve a desired apoapsis altitude. Most of these techniques rely on high dynamic pressures to realize the necessary drag. As a consequence, the heating rates of these techniques are also quite large, forcing the spacecraft to carry massive heatshields to protect the spacecraft during the aerocapture drag pass. If instead, the spacecraft had a large frontal projected area, then the same drag deceleration could be achieved by flying at a higher altitude, and thus at a lower dynamic pressure and heating rate. One manner of achieving a low dynamic pressure aerocapture is by deploying a ballute (a combination of a balloon and a parachute) that trails behind the spacecraft.[1–4] Because of the low heating rates, the constraints on the spacecraft design are much reduced and a maqssive heatshield is unnecessary. The ballute aerocapture possibility offers another attractive advantage: Once the desired drag deceleration has occurred, the ballute can be released from the spacecraft. Since the large ballute is responsible for most of the incurred drag loss, releasing it provides the aerocapture system with a measure of control. The problem now becomes one of finding a robust control that relaxes the other requirements of the aerocapture drag pass, particularly the approach navigation delivery error and the knowledge of the atmospheric density. Previous work on ballute aerocapture at Titan indicated one promising trigger, which releases the ballute when some specified function of two observable parameters (in this case, integrated drag delta-V and maximum observed drag deceleration) was met.[5] This study uses a higher fidelity model, by incorporating both latitudinal (zonal) variations as well as random perturbations in the TitanGRAM atmospheric density model.[6]

Figure 1 illustrates the major events during an aerocapture drag pass. The spacecraft arrives at Titan on an inbound hyperbolic trajectory, targeting the proper entry conditions for the drag pass, with the ballute already inflated. After entry, the spacecraft collects accelerometer measurements and determines the proper time to release the ballute. Once the ballute has been released, the spacecraft's ballistic coefficient

*Senior Engineer, Mission Design and Navigation, 4800 Oak Grove Dr., Pasadena, CA, 91109-8099, Member AIAA.

is dramatically increased, and ascends out of the atmosphere, encountering minimal drag on the way out. Once out of the atmosphere, the spacecraft orbit is circularized to the desired science orbit.

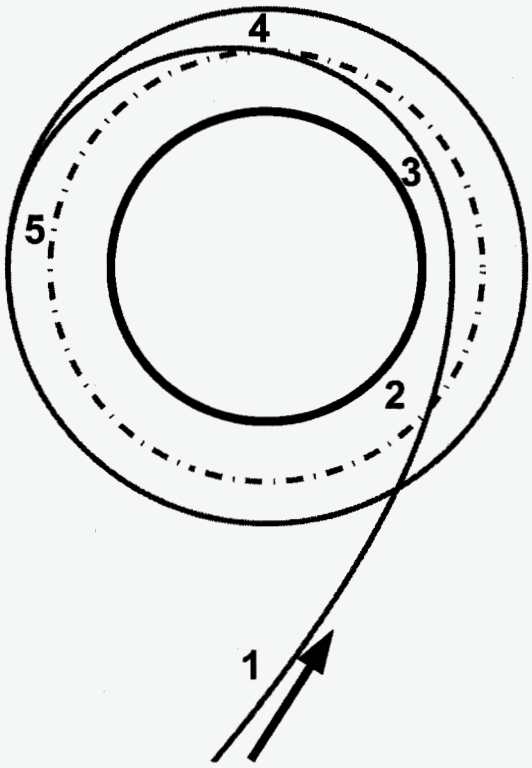

Figure 1. The aerocapture drag pass. (1) Spacecraft descends towards Titan towing the inflated ballute. (2) Atmospheric entry. (3) Onboard separation trigger releases ballute. (4) Atmospheric exit. (5) At apoapsis, spacecraft raises periapsis (and eventually establishes the specified orbit for the science mission).

II. Simulation Models

A. Spacecraft

The aerocapture maneuver is less susceptible to errors as the difference in ballistic coefficients between the orbiter and the ballute increases. In the ideal case, the orbiter would have a ballistic coefficient of infinity, so that when the ballute is released from the orbiter, the orbiter would immediately be on a drag-free Keplerian orbit out of the atmosphere. Since increasing the orbiter's ballistic coefficient to an absurdly high value is impractical, we concentrate on decreasing the ballistic coefficient of the ballute, by using as large of a ballute as is practical. However, increased ballute area leads to increased ballute mass, which must initially be carried by the orbiter. We use the same spacecraft properties as a previous study,[5] which sized the ballute to a feasible intermediate value (not too small to be ineffective, and not too large as to be unwieldy). The spacecraft properties are shown in Table 1. As with the previous study, we assume constant drag coefficients.

Table 1. Spacecraft properties.

Property	Value
Orbiter+Ballute frontal area	750 m^2
Orbiter+Ballute drag coefficient	1.37
Ballute mass	42.4 kg
Orbiter mass	457.6 kg
Orbiter frontal area	3 m^2
Orbiter drag coefficient	1.1

B. Atmosphere

TitanGRAM currently uses a single parameter, Fminmax, to allow the user to interpolate between three reference atmospheric profiles. An Fminmax=-1 corresponds to the thinnest atmosphere believed possible, 0 corresponds to the nominal profile, and +1 corresponds to the thickest atmospheric profile. There are no latitudinal, seasonal, or diurnal effects in the current beta version of TitanGRAM. The extremes of these parameters are all lumped together in the Fminmax parameter. The previous study assumed that a constant Fminmax accurately described the atmosphere observed throughout the aerocapture trajectory.

One model for Fminmax that accounts for latitudinal variability is shown in Eq. 1:[7]

$$Fminmax = A\sin(\text{lat}) + B \tag{1}$$

where

$$A \approx 0.46 \tag{2}$$

$$B \sim \text{Uniform}[-0.54, +0.54] \tag{3}$$

The parameters A and B are chosen to constrain Fminmax to within ± 1, with a weighting on the denser part of the atmosphere being in the north polar region for the arrival date associated with this particular mission scenario.

Given an Fminmax parameter, and an altitude, TitanGRAM provides (among other outputs) the nominal density that is used in the simulation. We model noise by applying a random, time-varying multiplicative scaling factor to this nominal density. In the Monte Carlo runs, we let the time interval between independent samples of the noise function vary uniformly between 1 sec and 20 secs. The scaling factor is assumed to vary linearly between independent samples.

C. Navigation

We used a previously generated set of 2001 dispersed entry states for another Titan aerocapture mission concept.[8] Since these entry states were intended for an aerocapture vehicle using a heatshield at high dynamic pressures, we adjusted the states by increasing the osculating periapsis altitude uniformly such that the expected 3σ worst case entry state coupled with the thinnest atmosphere would barely capture the spacecraft without ever needing to release the ballute.

These states correspond to a trajectory that arrives over the Titan north pole and enters the atmosphere in a southwesterly direction. With the Fminmax model in Eq. 1, the spacecraft would enter the atmosphere in the relatively thickest portion at some maximum value of Fminmax, and fly its way out with a continuously decreasing Fminmax parameter. The results of the constant Fminmax study[5] demonstrated that the ballute separation algorithm was more robust to an atmosphere characterized by a low Fminmax parameter. The reasoning is that the percentage of the aerocapture drag pass with the ballute still attached increases as the

drag deceleration decreases. When the ballute is finally released after passing through a thin atmosphere, the spacecraft has already ascended from periapsis, and not much time remains for the atmosphere to act upon the orbiter. A decreasing Fminmax parameter pronounces this effect even further. Most of the drag occurs before periapsis, and then the deceleration slows down and is more evenly spread across the remainder of the drag pass. Thus, timing errors have less of an effect on the atmospheric exit conditions (when A is large in Eq. 1).

III. Ballute Separation Triggers

The spacecraft accelerometer can provide total deceleration (integrated ΔV) as well as the rate of deceleration (g-load experienced by the spacecraft). We want the spacecraft to release the ballute once the proper deceleration is reached. Since the post-separation trajectory is not completely drag-free, the ballute separation trigger should account for the expected drag after separation. In the case where the atmosphere is thicker than expected (or periapsis is lower than expected), the g-loads will reach a higher maximum. In order to obtain the desired atmospheric exit conditions, the ballute is separated earlier than normal, so that the orbiter by itself is sufficient to obtain the remaining needed deceleration. Conversely, a thin atmosphere (or a high inbound periapsis case) will require the ballute to separate at a later time, when the g-loads are lower.

The trigger law in the previous study said that the ballute should be released from the spacecraft when the integrated ΔV of the drag pass exceeded a polynomial function of the maximum observed g-load. However, atmospheric perturbations will cause the instantaneous g-load to vary away from the nominal value. The performance of a trigger with the maximum observed g-load as the independent variable will depend greatly on the specific perturbations experienced by the spacecraft. An approach to alleviate this problem is to smooth out the noisy deceleration measurements by some appropriate filter prior to use by the trigger.

Another possible modification to the trigger is to use the (smoothed) instantaneous g-load as opposed to the maximum observed (smoothed) g-load. There are several different smoothing filters that can be used, but all will essentially be averaging the observed data (regardless of whether it uses an exponential weighting factor, or if its a simple moving average filter). For convenience, we restrict this study to the moving average filter.

The remaining choice to make is the length of the filter. A longer filter will provide more smoothing capability, and the filter length should be longer than the expected wavelength in the density waves. Furthermore, the filter should be causal, since it must operate in real-time. We note that a smoothing filter essentially integrates the g-load over its window. So instead of the independent parameter of the polynomial trigger law being "instantaneous g-load", it would be "integrated ΔV over the last n seconds". But the dependent variable of the polynomial is already integrated ΔV!. If the filter length is picked too large, the trigger law will become a truth statement. In other words, any set of inputs will always cause the trigger to fire. For this reason, we do not want to pick a filter length that is too large – the filter length should be long enough to smooth expected density waves, but no longer.

We propagate several trajectories that release the ballute at the correct time (such that upon exit, the spacecraft achieves the desired 1700 km apoapsis target) using a spread of smooth atmospheres (multiplicative noise factor is not applied) and a spread of inbound periapsis altitudes (the extreme low case, the nominal case, and the extreme high case). Since Fminmax varies with latitude, we use the bias term, (B from Eq. 1) to denote which atmosphere is being used. We can then filter the results according to the chosen trigger, and obtain a polynomial to use in the Monte Carlo trials.

Figures 2(a) and 2(b) depict the appropriate (g-load,ΔV) pair for a nominal case which precisely achieves the desired exit condition, and the best-fit 5th degree polynomial that interpolates the points. There are 93 pairs of (g-load,ΔV) points from which the polynomials are generated. These points correspond to 31 different Fminmax biases, and 3 different inbound periapsis altitudes. The left-hand most points correspond to low Fminmax biases (thin atmospheres), while the right-hand most points correspond to high biases (thick atmospheres). In Fig. 2(b), the upper points correspond to the extreme low delivery periapsis altitude, while

the lower points correspond to the extreme high delivery periapsis altitude. We note that the length of these curves is primarily due to the variation in the Fminmax parameter. If the atmosphere of Titan were better known, the curves in Figs. 2(a) and 2(b) would shrink. However, since the entry states are targeted so that the "thinnest" atmosphere would still allow capture, the part of the curves that would shrink would be the right side, and not the left. The left-hand side of the curve is the ideal area in which the triggers could operate, since it is relatively flat – the proper ballute separation time for these cases is towards the end of the aerocapture drag pass, and the remainder of the drag pass would be too short for any further perturbations to significantly affect the trajectory.

When we use the smoothed g-load as the independent variable [Fig. 2(a)], we discover that the Fminmax bias term is the only determining factor for generating the polynomial. The inbound periapsis altitude does not produce a spread of the nominal (g-load,ΔV) points, as is the case when using the maximum of the smoothed g-load trigger[5] [Fig. 2(b)].

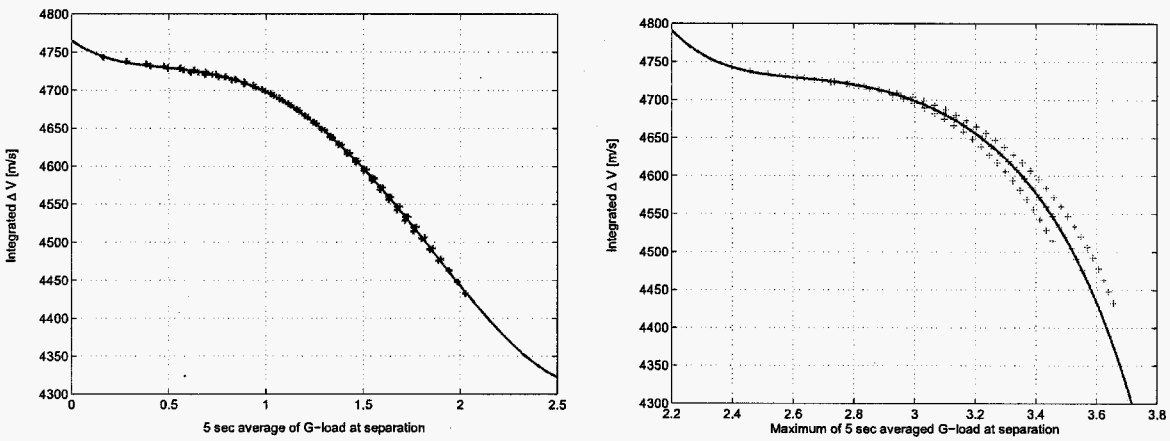

(a) (b)

Figure 2. Polynomial control laws for the cases with the g-load preprocessed by a 5 second moving average filter. The blue plusses indicate a (g-load,ΔV) pair for nominal cases that precisely achieves the desired exit condition. The red curve indicates the polynomial that interpolates between the data points.

Figures 3(a) and 3(b) depict the appropriate (g-load,ΔV) pair for a nominal case which precisely achieves the desired exit condition, for a variety of filter lengths. A nominal trajectory (i.e., one in which the exit conditions achieve a desired 1700 km apoapsis) has a ballute separation time after reaching the peak dynamic pressure. As the filter length increases, the time-averaged g-load also increases, as the beginning of the filtering window moves backwards in time. The typical ballute separation time is around 120-150 seconds after peak dynamic pressure. Thus, a filter length of 120-150 secs will result in a decreasing nominal, time-averaged separation g-load [in Fig. 3(a)]. Since most of the ΔV of the aerocapture pass occurs around the peak dynamic pressure, any filter length of 120-150 seconds or larger will cause the problem mentioned earlier of the trigger law becoming a truth statement. We thus only consider filter lengths less than 120 seconds.

The trigger law derived from the points in Fig. ??(b) suffer from a similar problem of increasing the filter length. Since the x-axis represents the maximum of the time-averaged g-load, then once the peak dynamic pressure is reached, the maximum g-load the spacecraft has experienced thus far becomes constant. Thus, a time history of (g-load,ΔV) for a case will terminate in a vertical line that intersects the trigger curve. The 180 second filter (orange points) is useless, since the law can not distinguish between points that should trigger early or late. The high filter length cases should be avoided in any case, since those curves become fairly steep. A small error in measured maximum g-load results in a large error in the integrated ΔV (and

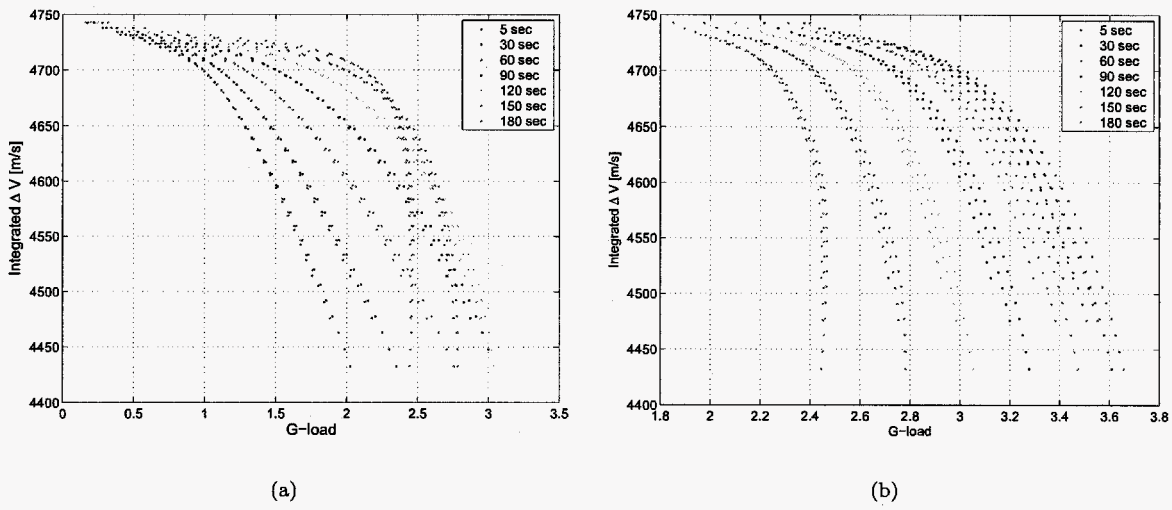

Figure 3. Data points for moving average filter lengths of 5, 30, 60, 90, 120, 150, and 180 seconds. The points indicate a (g-load,ΔV) pair for nominal cases that precisely achieves the desired exit condition.

thus, time) for ballute separation.

Combining the two choices for independent variable (the filtered instantaneous g-load, or the maximum of the filtered instantaneous g-load), and the two choices for filter length (5 secs or 90 secs, we have a total of 4 control laws which are considered in the results that follow.

IV. Results

A. Smooth Atmospheric Cases

For a smooth atmosphere, we can evaluate the performance of a trigger by determining the apoapsis altitude a trajectory achieves at atmospheric exit, as well as the ΔV required to circularize the orbit to 1700 km. Figures 4(a) - 4(d) illustrate the performance of both types of triggers (filtered g-load trigger, or maximum of filtered g-load trigger) across a range of delivery states and a range of Fminmax biases (the B term from Eq. 1).

As shown in the previous section, the trigger polynomial using the smoothed g-load as the independent variable does not strongly depend on the inbound periapsis altitude. Thus, Fig. 4(a) and 4(c) illustrate ideal performance for all Fminmax and all periapsis altitudes.

When the trigger polynomial instead uses the maximum of the smoothed g-load history as the independent variable [Fig. 4(b) and Fig. 4(d)], the performance of the trigger is somewhat worsened for cases with both a high Fminmax bias and an inbound periapsis altitude away from 526 km (i.e., the targeted inbound periapsis).

B. Monte Carlo Results

The polynomial separation algorithms were evaluated using 2000 dispersed cases. Each case used a random sampling of the 2001 entry states, an Fminmax bias uniformly distributed between -0.54 and +0.54, a time-varying density scale factor with a 3σ perturbation uniformly distributed between 0% and 50%, and whose sample time is uniformly distributed between 1 sec and 20 secs. The density scale factor is linearly

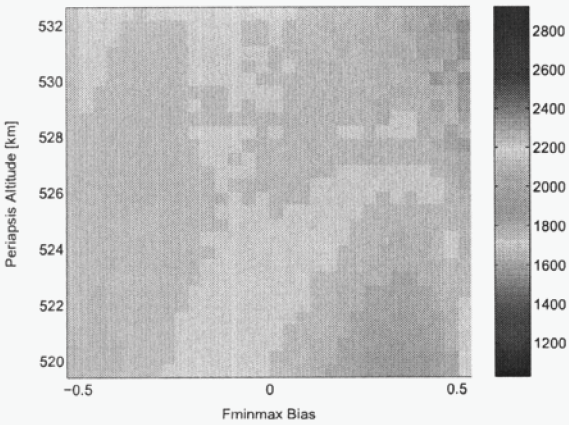

(a) Apoapsis altitude at atmospheric exit using 5-second smoothed g-load

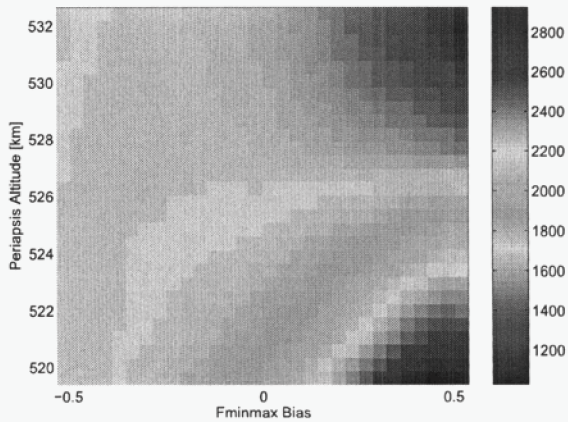

(b) Apoapsis altitude at atmospheric exit using maximum of 5-second smoothed g-load

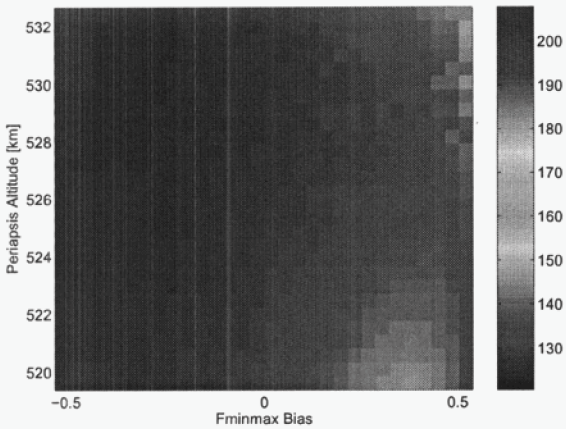

(c) ΔV required to circularize to 1700 km orbit using 5-second smoothed g-load

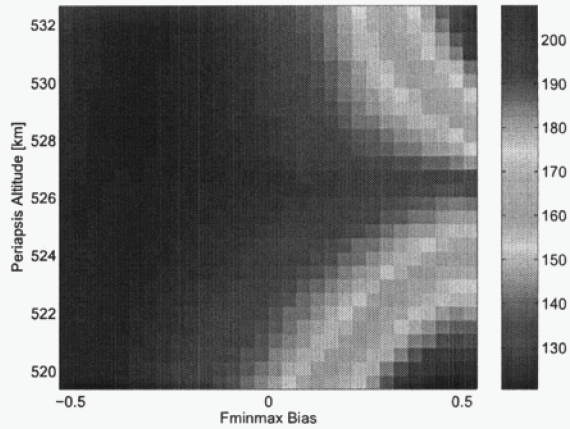

(d) ΔV required to circularize to 1700 km orbit using maximum of 5-second smoothed g-load

Figure 4. Performance of control laws using smooth atmospheres. The independent axes are the Fminmax bias, and inbound osculating periapsis altitude. In (a) and (b) the color represents the apoapsis altitude achieved (in km) at atmospheric exit. For (c) and (d) the color indicates the ΔV (in m/s) required to circularize orbit to 1700 km.

interpolated between adjacent samples. The trigger logic was evaluated at 10 Hz.

A summary of some Monte Carlo statistics is presented in Table 2. The cases with 90 second filters generally performed better than the 5 second cases. Because the assumed noise length tended be to longer than the 5 second filters, these cases were more easily spoofed by spurious noise. For the 5 second time-averaged filter case, the trigger polynomial tended to separate the chute too late, while the maximum of the 5 second filter case tended to separate too early. Both 90 second cases were less susceptible to noise, but 3.5% – 4.1% of the cases did not escape the atmosphere.

The failure cases could still be turned into successful aerocaptures. As soon as the spacecraft is able to determine that it will either not escape the atmosphere, or that it will not get captured by Titan, then the spacecraft could execute a propulsive maneuver to attain the necessary ΔV.

Histograms of the apoapsis altitude achieved after the aerocapture pass, and the necessary ΔV to circularize the orbit are shown in Figures 5 and 6 respectively. The ΔV is computed using 2 impulsive burns at the apsides.

Table 2. Summary of Monte Carlo Results.

Trigger Type	Time Averaged	Max of Time Averaged	Time Averaged	Max of Time Averaged
Filter Length	5 sec	5 sec	90 sec	90 sec
Mean Apoapsis	2062.5 km	6765.1 km	1799.4 km	1893.1 km
1σ Apoapsis	2002.5 km	32421 km	429.4 km	751.9 km
Mean ΔV^a	151.7 m/s	213.9 m/s	140.2 m/s	146.4 m/s
1σ ΔV^a	46.1 m/s	110.7 m/s	24.9 m/s	34.2 m/s
Number of cases (out of 2000) that...				
...crash before release[b]	59	0	0	0
...crash after release[c]	124	0	71	83
...fail to capture	0	44	0	0

[a] ΔV required to circularize the orbit to 1700 km

[b] The osculating apoapsis altitude decreased to be below the top of the atmosphere before the ballute was released.

[c] The osculating apoapsis altitude decreased to be below the top of the atmosphere after the ballute was released.

V. Conclusions

These triggers could be made more robust by combining them with other trigger options and using a "voting" scheme to select the ballute separation time. For example, one such other method could be to use onboard navigation that decides to release the ballute when the osculating apoapsis value reaches a certain point. Multiple polynomial-based triggers could be used (using different filter lengths, or one of each type [smoothed g-load vs maximum of smoothed g-load]).

The polynomial-based trigger schemes for ballute separation yield good performance, but with room for improvement. The biggest improvement would come from reducing the uncertainty in the Titan atmospheric model. Although this technique allowed a wide range of the atmospheric density profile (via the TitanGRAM Fminmax parameter, and the noise perturbations), the general structure of the atmosphere was assumed known. Cassini-Huygens, now orbiting Saturn, have the potential to increase our understanding of the Titan atmosphere, and reduce the modeling uncertainties.

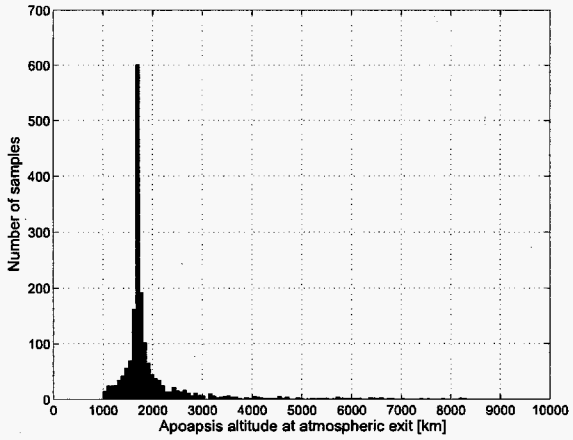

(a) Histogram for 5 second smoothed g-load

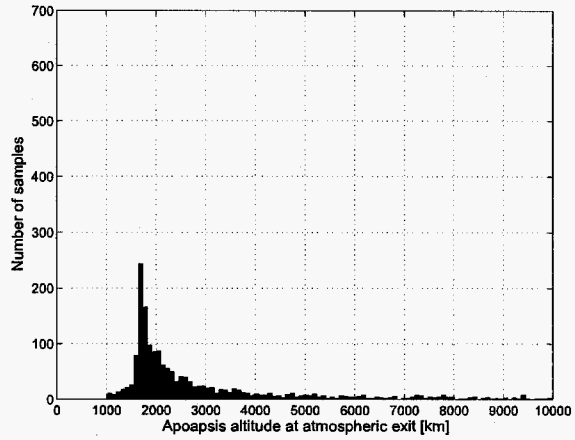

(b) Histogram for maximum of 5 sec smoothed g-load

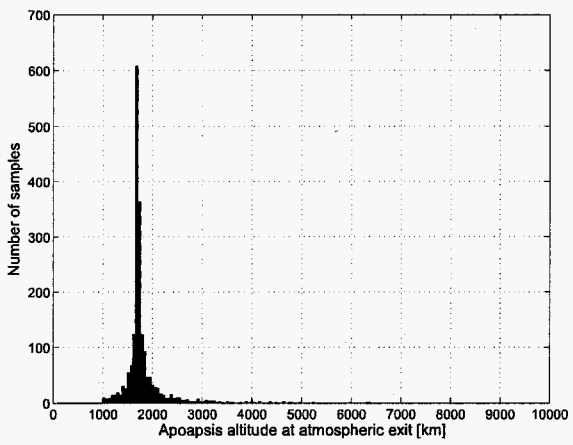

(c) Histogram for 90 second smoothed g-load

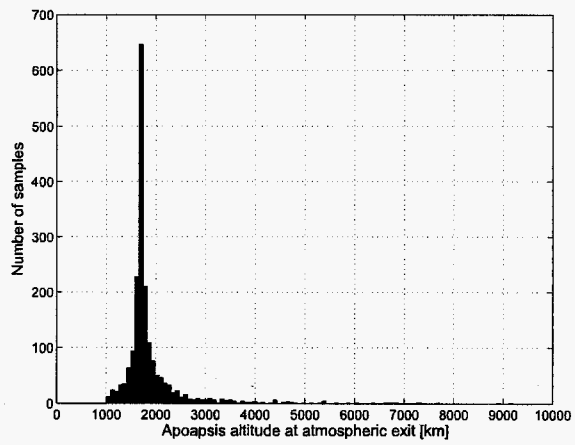

(d) Histogram for maximum of 90 sec smoothed g-load

Figure 5. Histograms of achieved apoapsis after an aerocapture through a noisy atmospheres.

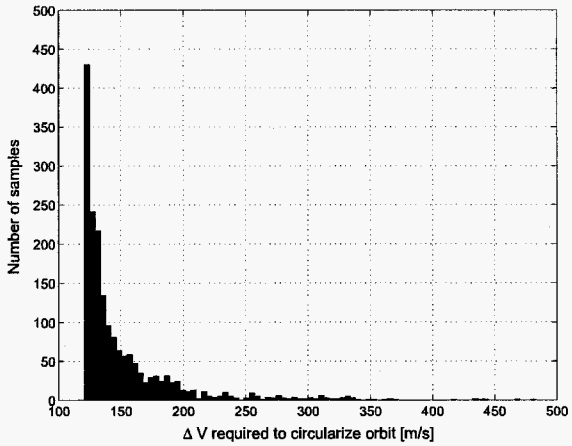

(a) Histogram for 5 second smoothed g-load

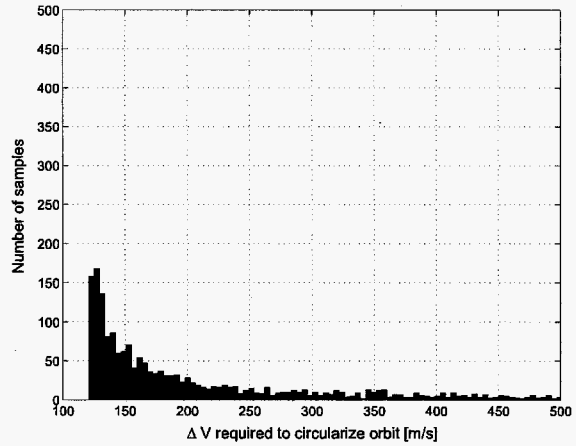

(b) Histogram for maximum of 5 sec smoothed g-load

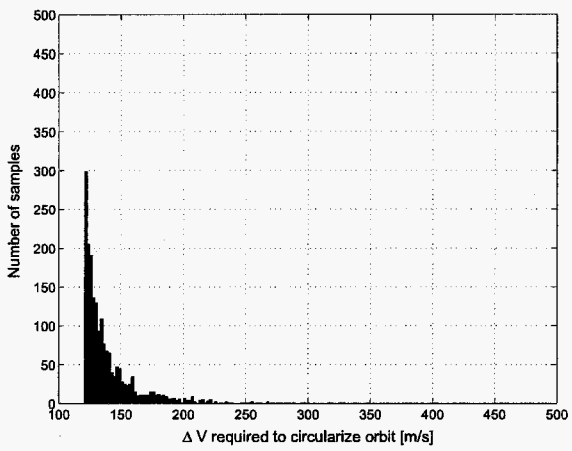

(c) Histogram for 90 second smoothed g-load

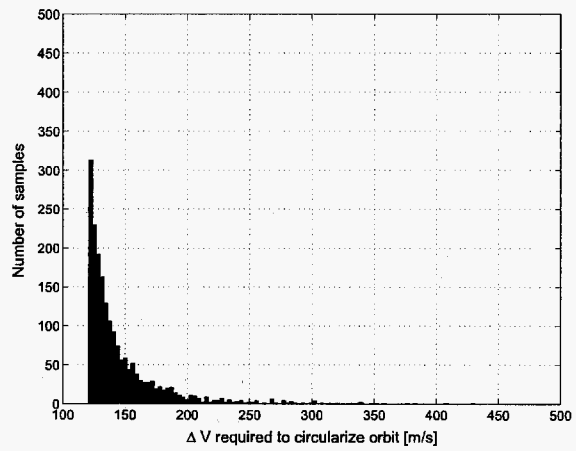

(d) Histogram for maximum of 90 sec smoothed g-load

Figure 6. Histograms of ΔV required to circularize orbit after an aerocapture through a noisy atmosphere.

VI. Acknowledgments

The research described in this paper was carried out by the Jet Propulsion Laboratory, California Institute of Technology, under a contract with the National Aeronautics and Space Administration. Funding for this study was provided by the NASA Office of Space Science through the In Space Propulsion Program. The authors would particularly like to thank the trailing ballute Principal Investigator, Kevin Miller (Ball Aerospace) as well as Bonnie James, Michelle Munk, and Erin Richardson at the NASA Marshall Space Flight Center, In Space Propulsion Program office for their sponsorship and excellent guidance in the management of these efforts.

References

[1]McRonald, A., "A Light-Weight Inflatable Hypersonic Drag Device for Planetary Entry," *Association Aeronautique de France Conference*, Arcachon, France, Mar 16-18 1999.

[2]McRonald, A., "A Light-Weight Inflatable Hypersonic Drag Device for Venus Entry," *AAS/AIAA Astrodynamics Specialist Conference*, Girdwood, Alaska, Aug 16-19 1999, AAS 99-355.

[3]McRonald, A., "A Light-Weight Inflatable Hypersonic Drag Device for a Neptune Orbiter," *AAS/AIAA Spaceflight Mechanics Conference*, Clearwater, Florida, Jan 23-26 2000, AAS 00-170.

[4]Hall, J., "A Review of Ballute Technology for Planetary Aerocapture," *4th IAA Conference on Low Cost Planetary Missions*, Laurel, MD, May 2–5 2000.

[5]Lyons, D. and Johnson, W., "Ballute Aerocapture Trajectories at Titan," *AAS/AIAA Spaceflight Mechanics Conference*, Aug. 2003, AAS Paper No 03-646.

[6]Justus, C., "TitanGRAM beta version on CD," Personal Communication.

[7]Justus, C., "Fminmax as a function of latitude," Personal Communication.

[8]Haw, R., "Approach Navigation for a Titan Aerocapture Orbiter," *AIAA/AAS Joint Propulsion Conference*, Huntsville, AL, July 20-23 2003, AIAA 2003-4802.